



CFD simulation optimization of a swirling vortex cavitator and its oxytetracycline degradation characteristics: kinetics and degradation pathway

Baoe Wang^a, Rihong Zhang^{b,*}, Yiyong Li^a, Xiaoming Lian^a

^aCollege of Resource and Environment, Zhongkai University of Agriculture and Engineering, Guangzhou 510225, China, emails: baowang@163.com (B. Wang), 350527256@qq.com (Y. Li), 463985047@qq.com (X. Lian)

^bCollege of Mechanical and Electrical Engineering, Zhongkai University of Agriculture and Engineering, Guangzhou 510225, China, Tel.: +86 2036078375; email: zrh-neu@163.com (R. Zhang)

Received 6 November 2022; Accepted 10 February 2023

ABSTRACT

Vortex cavitation may be harnessed to intensify many industrial processes. It is essential to develop a highly efficient vortex cavitator for refractory organics degradation. In the present work, a novel swirling vortex cavitator designed with a special structure of six vortex cavities and spiral flow passages was optimized using computational fluid dynamics (CFD) method by the aid of Gambit software and ANSYS fluid simulation software, and its oxytetracycline degradation characteristics were investigated. The optimized vortex cavitator was superior to the original vortex cavitator resulting from more hydroxyl radicals generated during operation and higher oxytetracycline degradation efficiencies. The degradation efficiency was 89.52% and 92.41% of about 2.0 mg/L initial concentration of oxytetracycline in 10 L solution at 80 min by the original and optimized swirling vortex cavitator, respectively. The optimized vortex cavitator also showed good oxytetracycline degradation ability in aquaculture simulation wastewater. All the degradation processes followed the second-order kinetics model. In the two degradation pathways, multiple by-products were generated by dealkylation, deamination, dihydroxylation and ring-opening induced by vortex cavitation effect.

Keywords: Swirling vortex cavitator; CFD simulation optimization; Degradation; Oxytetracycline

1. Introduction

Antibiotics are widely used in the prevention and treatment of infectious diseases in humans and animals. Studies have shown that antibiotics environmental pollution and ecotoxicological effects have become one of the major environmental problems of the world, with the mass production and widespread use of them [1]. Especially, more than 70% of oxytetracycline antibiotics are excreted and released in active form into the environment via urine and feces from humans and animals after medication. The antibiotics induce the emergence of drug-resistant pathogenic bacteria in the environment and poses a threat to human health and

ecological environment [2]. Most of these pharmaceuticals are stable and difficult to oxidize by conventional treatment processes. It is necessary to identify an effective and feasible technology for degrading oxytetracycline in water environments.

Hydrodynamic cavitation (HC) is a novel technique that has extensive applications, ranging from food processing, water sterilization to waste remediation [3]. Compared with other conventional AOP (advanced oxidation processes) wastewater treatment techniques, HC has proved to be characterized by greater pollutants removal efficiencies, lower energy requirements and fewer secondary contamination problems [4]. HC technology mainly includes

* Corresponding author.

the vortex cavitation technology and jet cavitation technology. The latter requires more complex equipment and more energy due to a high initial fluid velocity at the inlet of cavitator. Therefore, vortex cavitation technology will show greater application prospect in the treatment of toxic and refractory organic wastewater. However, jet cavitators with venturi tube structure are most used for degradation of refractory in many open literatures [5–8]. Only a few types of vortex cavitators have designed [9–11]. Moreover, the efficiencies of degradation of dyes, BTEX and other organic compounds by them are not ideal [11–13]. Thus, the design of a novel vortex cavitator and optimization the structure is the key to improve the degradation efficiency of refractory.

In the present work, the vortex cavitator structure parameters were simulated and optimized on the basis of a novel swirling vortex cavitator designed in our previous study [14]. Then, the hydroxyl radicals generated during operation and degradation efficiencies of oxytetracycline by the original and optimized vortex cavitator were compared. Further, the degradation kinetics and the possible degradation pathways were investigated. The concentration level of oxytetracycline present in the natural water bodies, WWTPs and antibiotics wastewaters can be varying from ng/L, µg/L to mg/L in sequence [15,16]. Thus, the initial concentration of 2.0 ± 0.04 mg/L selected may provide a new way for the treatment of antibiotic wastewaters in this study.

2. Materials and methods

2.1. Oxytetracycline

Oxytetracycline (OTC), $C_{22}H_{24}N_2O_9$, (Shanghai Yuanye Biotechnology Co., Ltd., China), is analytical pure 98%.

2.2. CFD simulation methods

2.2.1. Creation of 3D fluid model for vortex cavitation

Due to the software Creo's good compatibility with other 3D mechanical design software, the structural model of the swirling vortex cavitator was created by using Creo 3D design software. In order to facilitate the subsequent grid partitioning and simulation test, the file was saved in STP format. The "entity", "shell" and "small plane" were selected, which could prevent effectively the loss of small surface features in the output process of the model.

2.2.2. Mesh

Gambit software was used to import the STP format model file created above into Gambit file. The new entity created by the geometry model and the original model were computed by Boolean operation to obtain the fluid region.

2.2.3. CFD simulation models

The mixture model of multiphase flow model and realizable $k-\epsilon$ double-equation turbulence model were applied during CFD simulation. Cavitation effect was taken into account in the mass transfer process. The influence of temperature and the heat transfer process in the flow was ignored. The initial fluid state was assumed stationary.

2.2.4. Boundary conditions setting

The pressure inlet boundary condition was designated and the total pressure of the inlet was set as 0.3 MPa. The pressure outlet boundary condition was selected and the backpressure of the outlet was set as 0.0 MPa. The operating pressure was set as one bar pressure (101,325 Pa). The medium of the fluid was set as "water liquid".

2.3. Degradation experiments

2.3.1. Cyclic degradation process by swirling vortex cavitator

The degradation experiments equipment photo of Fig. 1 shows the cyclic degradation process. It is a closed loop system designed to pump 10 L of oxytetracycline solution from water tank, then take it into the swirling vortex cavitator and discharge the treated solution back to the water tank through the water pump. The inlet liquid pressure of the swirling vortex cavitator can be adjusted through regulation of the water pump outlet pressure.

2.3.2. Oxytetracycline degradation by swirling vortex cavitator

Oxytetracycline water solution or simulated aquaculture antibiotic wastewater of 10 L with an initial oxytetracycline concentration of 2.0 ± 0.04 mg/L at pH 7.0 was placed in the water tank. Four ice bags were placed to prevent the solution temperature from rising too high due to vortex cavitation effect. Then the water pump was started (the inlet pressure of the pump was set to be 0.15 MPa) and the degradation began. The ice bags were replaced at degradation time 10 min. The sample of 2.0 mL oxytetracycline solution was taken and filtered into the chromatographic bottle with 0.22 µm filter membrane for determination the concentration of oxytetracycline every certain time. After the degradation, rinsed the water pump and water tank three times with deionized water.

The simulated aquaculture antibiotic wastewater consists of $(NH_4)_2SO_4$ 135.0 mg/L, KH_2PO_4 91.0 mg/L, $MgSO_4 \cdot 7H_2O$

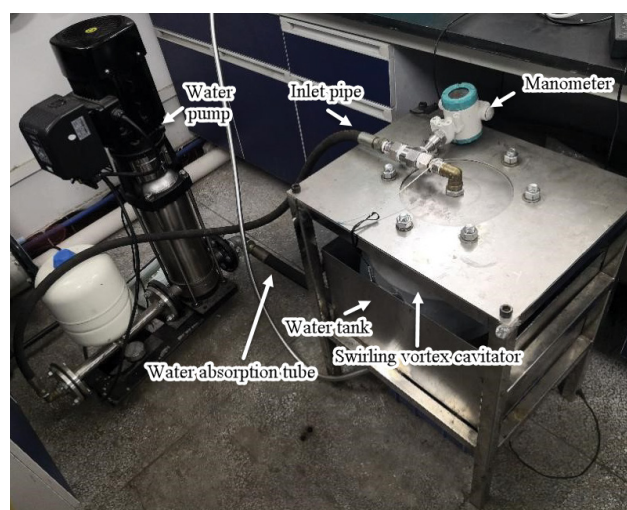


Fig. 1. Degradation experiments equipment photo.

95.0 mg/L, KCl 37.0 mg/L, Glucose 469.0 mg/L, and oxytetracycline 2.0 ± 0.04 mg/L.

All of the experiments were performed at least in triplicates.

2.3.3. Determination of hydroxyl radical concentration

Methylene blue method was used to determine the concentration of hydroxyl radical produced by the vortex cavitator [17], and the degradation steps were the same as above of oxytetracycline degradation, except the methylene blue solution instead of the oxytetracycline solution. The calculation formula of hydroxyl radical concentration is as follows:

$$C_{\cdot\text{OH}} = \frac{\Delta A}{0.07196} \quad (1)$$

where $C_{\cdot\text{OH}}$ is the molar concentration of hydroxyl radical, $\mu\text{mol/L}$. ΔA is absorbance difference of methylene blue in solution before and after degradation ($\lambda_{\text{max}} = 664 \text{ nm}$).

2.4. Analytical methods

The concentrations of oxytetracycline were analyzed by HPLC. It was performed in a WATER 2695 HPLC instrument using a Extend-C18 column (150 mm \times 4.6 mm, 3.5 μm particle size). The intermediate products analysis of degradation was performed in an Agilent 1290/6470 HPLC-MS instrument using an Agilent column (50 mm \times 4.6 mm, 2.1 μm particle size). The spectrometry analysis software was Smart Dalton HR software (Guangzhou Molecular Information Company). NIST2020, Wiley11 and Elsevier databases were used for spectral comparison.

2.5. Degradation efficiency

The degradation efficiency of oxytetracycline, X , was calculated by the equation as follows:

$$X = \frac{C_0 - C_1}{C_0} \times 100\% \quad (2)$$

where C_0 is the initial concentration of oxytetracycline, mg/L. C_1 is the concentration of oxytetracycline after degradation, mg/L.

3. Results and discussion

3.1. Cavitation effect formation analysis of the swirling vortex cavitator

Three-dimensional structure of parts of vortex cavitator is shown in Fig. 2. It can be clearly seen the distribution and assembly fit relationship of the upper end cover, vortex cavitation part and lower baffle plate. In order to make the small bubbles generated in the fluid collapse as much as possible and produce cavitation effect effectively, six vortex cavities are designed in this swirling vortex cavitator. The present vortex cavitators represent improvement and modifications of that of the literatures [9,10].

However, embodiments disclosed here have different configurations and modes of operation, which have been found to enhance the vortex effect.

The original structural sizes of vortex cavitator parts are the diameter of vortex cavity 65 mm, the gap width 5 mm, the diameter of spiral flow passage entrance 9 mm, and the outlet diameter of spiral flow passage 3 mm. There are four channels of 1 mm diameter leading to the jet cavity on each helical flow channel, enabling it to produce more cavitation times. Eight DN 12 bolt thread holes are distributed around the edge of the swirling vortex cavitation part for bolt connection with the upper end cover and tray. Six M8 threaded holes are evenly distributed at the bottom of the vortex cavitation part for connecting with the lower baffle plate.

The cavitation process is analyzed as follows: The fluid enters and diverges the center of the vortex cavitation part through the upper entrance of the upper end cover. Flowing through the small gap at the central edge of the vortex cavitation component, the fluid will generate large inlet velocity and enter tangentially the respective vortex cavity [9]. The fluid will swirl around the vortex chamber, creating a low-pressure region in the center of the vortex chamber [10]. The fluid then flows into the spiral channel. The cross-sectional area of the spiral channel gradually decreases along the way, resulting that the speed of the fluid gradually increases by the hydraulic principle. According to Bernoulli equation we know that it will produce a low-pressure area inside fluid. The low-pressure area will make the gas originally dissolved in the fluid overflow, forming small cavitation bubbles, which are the key to cavitation formation. With the loss of the fluid pressure, originally formed small cavitation bubbles will increase inflation. When the fluid comes out from the small orifice in the spiral channel, a dramatic increase in sectional area, which result in high pressure to squeeze the cavitation bubbles until they burst. At the same time, after the fluid in the vortex cavity comes out from the small orifice in the spiral channel, the fluid will move towards the center of the jet cavity. Multiple streams converge in the center of the jet cavity and can collide with each other to improve the bubble burst and cavitation effect. Thereafter, the fluid will strike the lower baffle plate strongly. It can increase the bubbles breaking and vortex cavitation effect, which can accompany

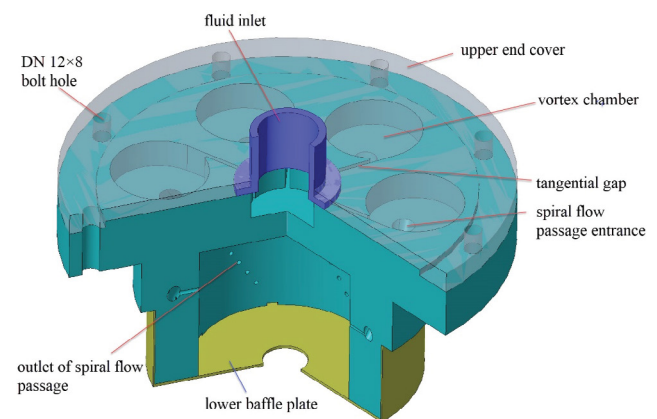


Fig. 2. Three-dimensional structure of the swirling vortex cavitator.

with huge energy released in the cavitation process. At last, the fluid motion potential energy is reduced, and flow from the exit at the bottom of the center of the lower baffle plate. Until this moment, the whole process of cavitation complete.

3.2. Results of meshing

The vortex cavitation flow regions were meshed by the aid of CFD pro-processing software Gambit. In order to capture the flow details and the cavitation area, the grids were dense and small size in the region of severe changes in geometry and of probable cavitation generating. The grids were large a bit in the region of not severe changes in the flow. In order to ensure the calculation accuracy as far as possible, and to reduce the number of grids and save the calculation time, the overall flow area was meshed by non-structural grids. The wall was set boundary layer grids. The meshing result is displayed in Fig. 3.

The total number of grids is 2,124,961. The Minimum Orthogonal Quality is 0.45. The maximum aspect ratio is 3.6. It achieves a good quality of mesh.

3.3. CFD simulation analysis of the original swirling vortex cavitator

One of the necessary conditions for vortex cavitation effect is the formation of low-pressure area. As long as the low pressure is lower than the saturated vapor pressure of the fluid, cavitation bubbles release. Thus, the fluid pressure of key components of original vortex cavitator was simulated by ANSYS software in this study. The cell Reynolds numbers of fluid region in the vortex cavitator is displayed in Fig. 4, and the fluid pressure distribution is shown in Fig. 5.

Fig. 4 displays that the cell Reynolds numbers varied in the range of $5.66 \times 10^{-3} - 5.08 \times 10^3$, indicating that drastic flow state changes occur in the vortex cavitator. There are the maximum cell Reynolds numbers at the entrance and orifice of the spiral flow passage. Generally speaking,

the fluid is turbulent with the Reynolds number of water exceeding 2×10^3 . The flow state of most area from the vortex chamber to the spiral flow passage outlet are turbulent.

Fig. 5 appears that low pressure areas are mainly distributed in the spiral flow passage. The minimum absolute pressure of the fluid was approximately 5,465.7 Pa. Temperature of tests was controlled under 55°C, at which the saturated vapor pressure of pure water is 15,737 Pa. Therefore, the produced minimum pressure value of vortex cavitator was much lower than the saturated vapor pressure at temperature, a certain number of vortex bubbles appeared simultaneously. After the bubbles rushed out of the flow channel exit, where the sectional area surged, resulting in outside pressure of bubbles increase. The cavitation effect forms after the bubbles collapsed due to inside and outside pressure difference of them.

3.4. CFD simulation optimization of the swirling vortex cavitator structure parameters

It would cause many experiments and low efficiency if the traditional permutation and combination method

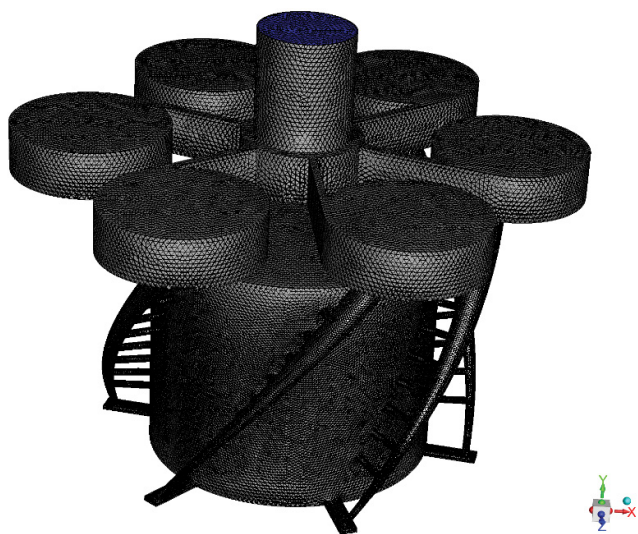


Fig. 3. Meshing result by the aid of Gambit software.

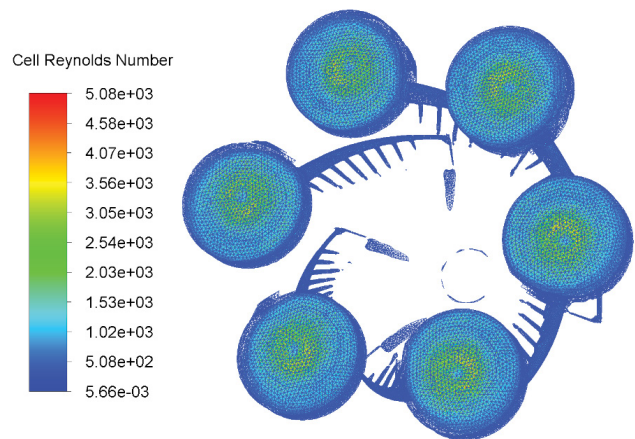


Fig. 4. Cell Reynolds number of fluid region.

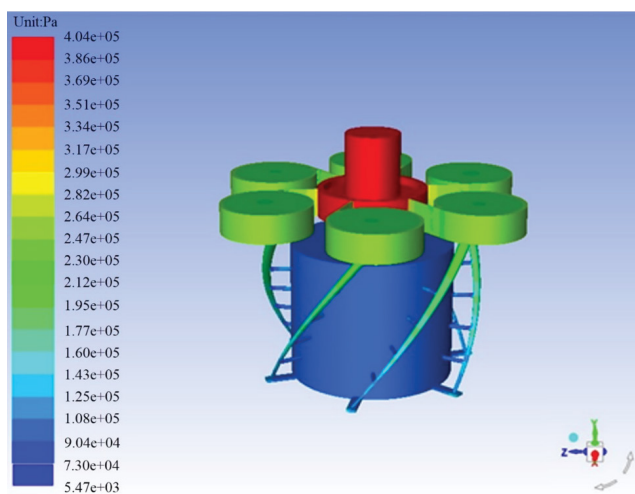


Fig. 5. Fluid pressure cloud diagram of the original swirling vortex cavitator.

is used to optimize the structure. Orthogonal experimental design is based on a design method of multi-factor and multi-level. It is to select some representative factors for the test from the overall tests according to the orthogonality. It can reduce the experiments times. Therefore, the orthogonal test was used to optimize the structural parameters of swirling vortex cavitator.

The gap width, the inlet diameter of spiral flow passage, the number of holes in each vortex chamber and the number of holes in spiral flow passage were selected as the optimization factors. The structural parameters of swirling vortex cavitator were simulated and optimized by orthogonal test method. The inlet pressure was set at 0.3 MPa. $L_9(3^4)$ orthogonal experiment was designed, and the factors and levels are listed in Table 1.

According to the orthogonal tests, the optimal structural combination was obtained. That is, the number of holes in the vortex cavity is 1, the number of holes in spiral flow passage is 5, the gap width is 6 mm, and the inlet diameter of spiral flow passage is 9 mm. It was simulated and verified the optimal parameter combination, and the minimum absolute pressure of the vortex cavitator with optimal structure combination was 5,150.14 Pa, as shown in Fig. 6. Compared with the 5,465.7 Pa before optimization, the minimum absolute pressure of the optimal structure reduced. It can expect that vortex cavitation effect will occur more easily.

3.5. Comparison of hydroxyl radical concentration generated by the original and optimized swirling vortex cavitator

Direct hydroxyl radical ($\cdot\text{OH}$) quantification is unlikely due to their high reactivity and short life-time (circa 10^{-9} s) [18]. Methylene blue method was used to quantify $\cdot\text{OH}$ indirectly in this study. Methylene blue concentration was 14.97 mg/L. The $\cdot\text{OH}$ concentration generated by the original and optimized swirling vortex cavitator was compared and shown in Fig. 7. The detected $\cdot\text{OH}$ concentration by original and optimized swirling vortex cavitator was 4.56 and 5.52 $\mu\text{mol/L}$ at 50 min, respectively. They were far more than that reported by a Venturi cavitation device, which is less than 0.3 $\mu\text{mol/L}$ [17]. With the increase of time, the concentrations of $\cdot\text{OH}$ both increased shown from Fig. 7. The higher concentrations indicate the vortex cavitation effect improved after optimization.

3.6. Comparison of oxytetracycline degradation in solution by the original and optimized swirling vortex cavitator

Oxytetracycline degradation efficiencies in solution by the original and optimized swirling vortex cavitator are

Table 1
Factors and levels orthogonal table

Number of holes in each vortex chamber	Number of holes in spiral flow passage	Gap width (mm)	Inlet diameter of spiral flow passage (mm)
1	4	4	9
2	5	5	12
3	6	6	15

Note: One hole in each vortex chamber connects one spiral flow passage.

shown in Fig. 8. The degradation efficiency in solution was 85.37% and 90.29% by the original and optimized swirling vortex cavitator at 60 min, respectively. The degradation efficiencies of oxytetracycline are both higher than that by jet hydrodynamic cavitation reported by Wang et al. [19]. Combined the above results that the $\cdot\text{OH}$ concentrations and oxytetracycline degradation efficiencies are both increased, it proves the optimized swirling vortex cavitator is superior

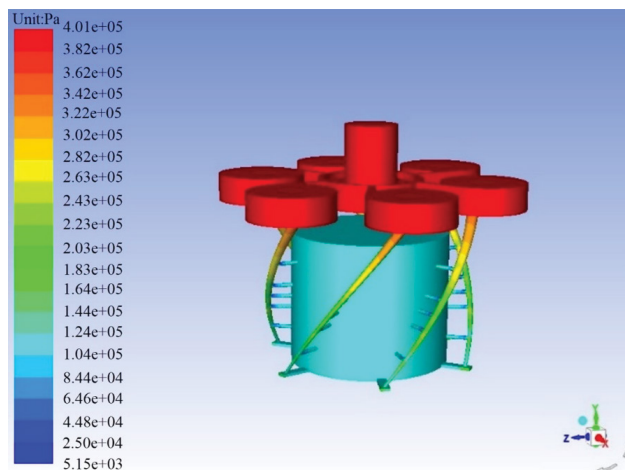


Fig. 6. Fluid pressure cloud diagram of the vortex cavitator with optimal parameter combination.

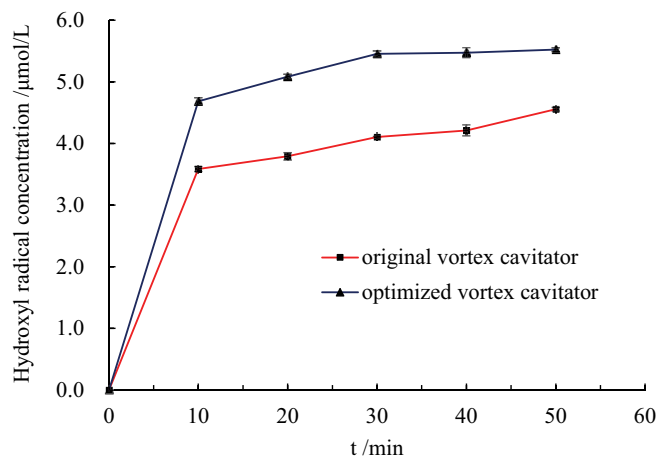


Fig. 7. Hydroxyl radical concentrations generated by the original and optimized swirling vortex cavitator.

to the original one. It also shows that the $\cdot\text{OH}$ concentration affects directly the degradation efficiency. The number of $\cdot\text{OH}$ is proportional to the number of cavitation bubbles collapsing. In the appropriate cavitation state, the more cavitation bubbles are generated and collapsed, the more energy is released, and the enhancement of cavitation effect accordingly.

Fig. 8 also displays that the degradation is fast in 10 min, then become slow gradually. It may due to the accumulation of intermediate products during the degradation process. Oxytetracycline is a macromolecular organic compound containing tricarbonyl amide, phenolic diketone and dimethyl amine groups [20]. The groups with high electron density are vulnerable to the attack of $\cdot\text{OH}$ in oxidation [21]. In the processes of cavitation degradation, the produced $\cdot\text{OH}$ can react with oxytetracycline and more and more accumulated by-products by cracking, hydroxylation and denitrification. It means need more and more $\cdot\text{OH}$ during the degradation, resulting in slower degradation.

3.7. Comparison of oxytetracycline degradation in aquaculture simulation wastewater by the original and optimized swirling vortex cavitator

In order to evaluate preliminarily the degradation efficiency in actual wastewater, the oxytetracycline degradation in aquaculture simulation wastewater by the original and optimized swirling vortex cavitator was studied. Fig. 9 displays that the degradation efficiency in aquaculture simulation wastewater was 71.15% and 76.7% by the original and optimized swirling vortex cavitator at 60 min, respectively. The degradation efficiencies in aquaculture simulation wastewater were lower than that in solution. It may be due to the interference from some reductive components in wastewater, such as glucose, ammonium sulfate. Nevertheless, the degradation efficiencies in aquaculture simulation wastewater exceeded 70% in 60 min, which means the good oxytetracycline degradation ability.

3.8. Degradation kinetics

In order to evaluate the kinetics of the cavitation degradation, the classical first-order kinetics model and second-order kinetics model usually are applied [22,23]. Compared with the correlation coefficient of fitting first-order model

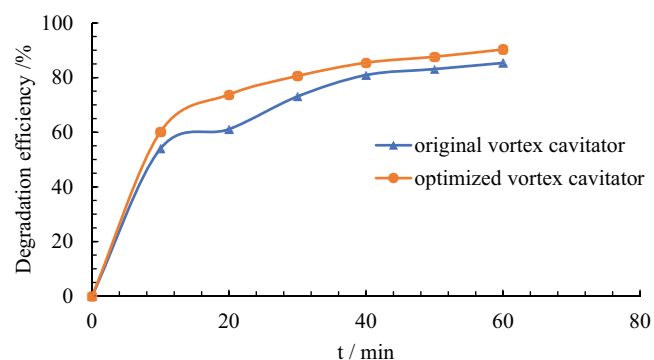


Fig. 8. Oxytetracycline degradation in solution by the original and optimized swirling vortex cavitator.

(R^2 range 0.8469–0.9297), the oxytetracycline degradation kinetics by original and optimized vortex cavitator reacted in solution and in aquaculture simulation wastewater all follows the second-order kinetics model ($R^2 > 0.97$), which is expressed as:

$$\frac{1}{C} = \frac{1}{C_0} + kt \quad (3)$$

where C is the oxytetracycline concentration at time t , k is the rate constant and t is the degradation time.

Mean square error (MSE) is calculated by the follow equation:

$$\text{MSE} = \sqrt{\frac{\sum (C_{\text{exp}} - C_{\text{cal}})^2}{N}} \quad (4)$$

where C_{exp} and C_{cal} is the oxytetracycline concentration of measured and that of calculated by the model, respectively. N is the number of oxytetracycline concentrations.

Fig. 10 shows the second-order kinetics fitted curves by the original and optimized swirling vortex cavitator in

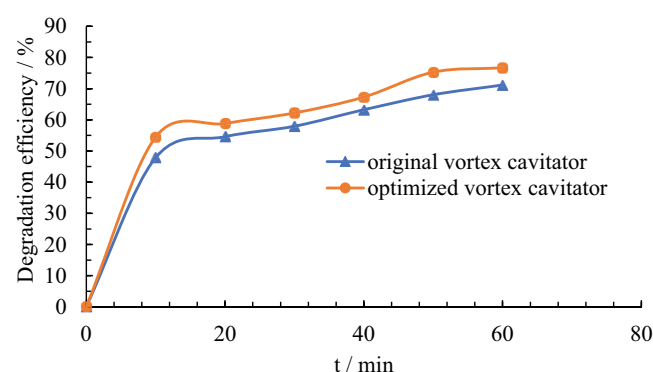


Fig. 9. Oxytetracycline degradation in aquaculture simulation wastewater by the original and optimized swirling vortex cavitator.

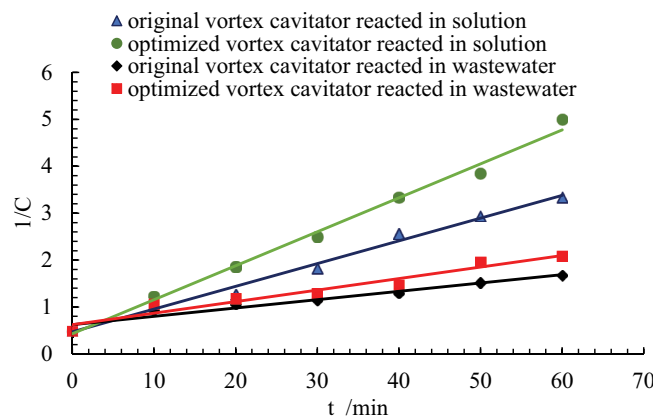


Fig. 10. Second-order kinetics fitted curves by the original and optimized swirling vortex cavitator reacted in solution and in aquaculture simulation wastewater.

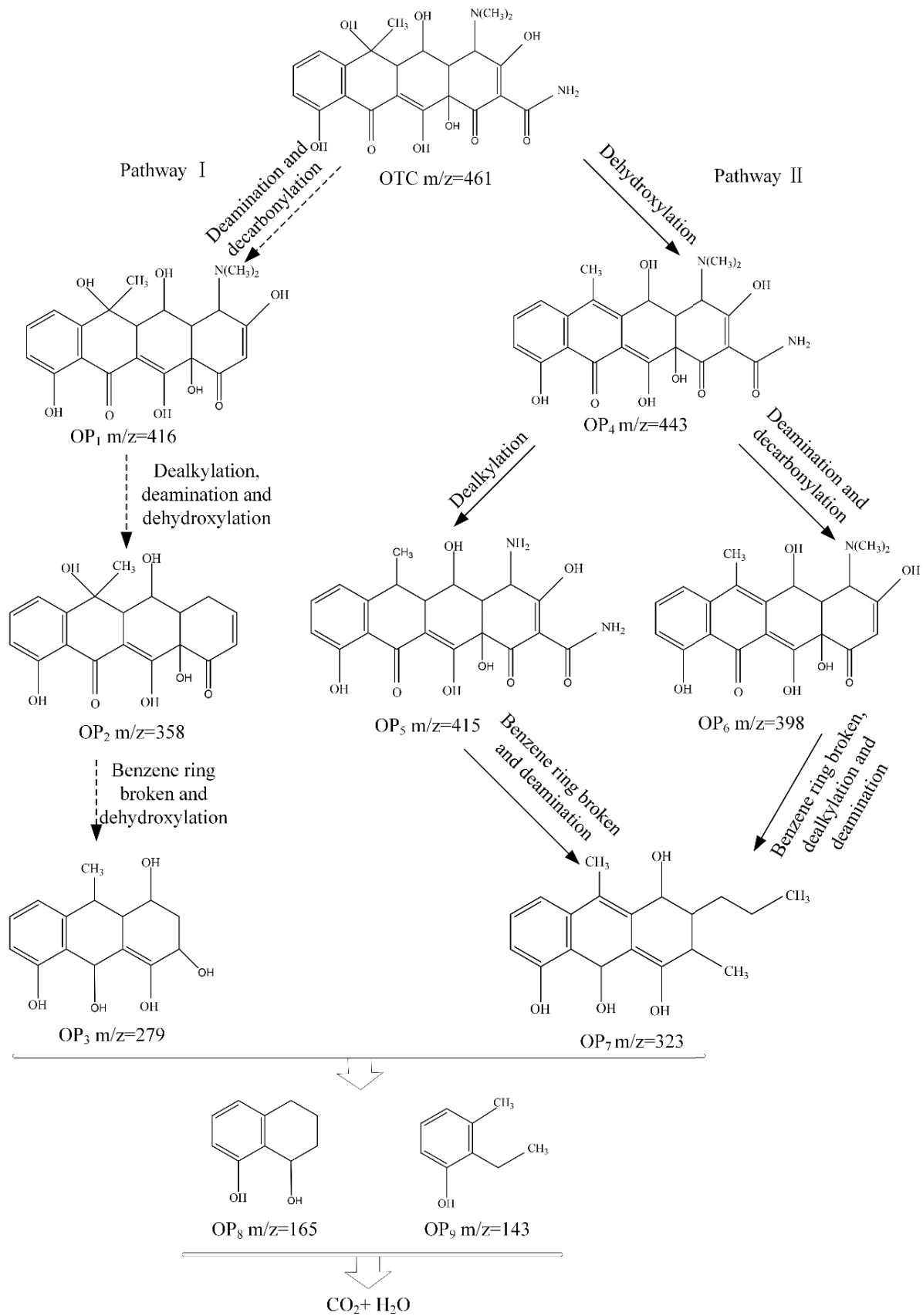


Fig. 11. Possible degradation pathways of oxytetracycline.

Table 2

Second-order kinetics simulation results and parameters by the original and optimized swirling vortex cavitator reacted in solution and in aquaculture simulation wastewater

Conditions	Equation	k (min ⁻¹)	R^2	MSE
Original vortex cavitator reacted in solution	$1/C = 0.0485t + 0.4689$	0.0485	0.9877	0.061
Optimized vortex cavitator reacted in solution	$1/C = 0.0724t + 0.4325$	0.0724	0.9925	0.021
Original vortex cavitator reacted in aquaculture simulation wastewater	$1/C = 0.0178t + 0.6227$	0.0178	0.9511	0.077
Optimized vortex cavitator reacted in aquaculture simulation wastewater	$1/C = 0.0246t + 0.623$	0.0246	0.9456	0.094

solution and in aquaculture simulation wastewater. Table 2 lists second-order kinetics simulation fitted curve equations and parameters. MSE were all less than 0.1, indicating a high correlation between experiment and model values. The kinetics rate constants (k) values were 0.0178–0.0724 min⁻¹, and those of vortex cavitator reacted in solution were larger than in wastewater. It indicates that the degradations in solution are faster than in aquaculture simulation wastewater, and the degradation by optimized vortex cavitator reacted in solution is the fastest.

3.9. Degradation pathways

In the process of vortex cavitation, huge energies and large amounts of $\cdot\text{OH}$ are produced, which can react with oxytetracycline by cracking, oxidation reaction etc. To find out the possible degradation pathways, the intermediate products of oxytetracycline in optimized vortex cavitator were determined by HPLC-MS Spectrometry. Some new peaks appeared in the degradation intermediates, such as $m/z = 443, 416, 398, 415, 358,$ and 323 . The possible degradation pathways of oxytetracycline were proposed in Fig. 11.

In the pathway I, the byproduct OP_1 ($m/z = 416$) was identified as the deamination and decarbonylation of original OTC under large energy generated by vortex cavitation effect [24]. The OP_2 ($m/z = 358$) was formed from OP_1 via dealkylation, deamination and dehydroxylation [25]. A benzene ring broken and dihydroxylation occurred in the products OP_2 to obtain an intermediate of OP_3 ($m/z = 279$) [26]. In the pathway II, the transformation by-product OP_4 ($m/z = 443$) was generated from the original OTC due to the dehydration process [27]. OP_6 ($m/z = 398$) is the product of deamination and decarbonylation of OP_4 . At the same time, the dealkylation of OP_4 forms an intermediate with OP_5 ($m/z = 415$) [28]. OP_7 ($m/z = 323$) was detected by series of reactions like benzene ring broken, dealkylation and deamination by OP_5 and OP_6 [29]. In both pathways, OP_3 and OP_7 was continuously decomposed to aromatic compounds OP_8 ($m/z = 165$) and OP_9 ($m/z = 143$) [26]. With increasing reaction time, through oxidative decomposition and ring-opening reactions, the OP_8 and OP_9 were finally decomposed into H_2O and CO_2 .

4. Conclusions

The CFD simulation method can be applied in the optimization of the vortex cavitator. The optimized structure parameters are as follows: one hole in the vortex cavity, 5 holes in spiral flow passage, 6 mm of the gap width, and 9 mm of the inlet diameter of spiral flow passage.

The designed swirling vortex cavitator can produce vortex cavitation effect. The optimized swirling vortex cavitator and its oxytetracycline degradation ability is superior to the original swirling vortex cavitator. The detected $\cdot\text{OH}$ concentration by the original and optimized swirling vortex cavitator was 4.56 and 5.52 $\mu\text{mol/L}$ at 50 min, respectively. The maximum degradation efficiency in solution was 89.52% and 92.41% by the original and optimized swirling vortex cavitator, respectively. The degradation efficiency in aquaculture simulation wastewater was 79.80% and 85.20% at 80 min by the original and optimized swirling vortex cavitator, respectively. All the oxytetracycline degradation kinetics follow the second-order kinetics model.

The two degradation pathways could describe process of oxytetracycline degradation. Multiple by-products were generated by dealkylation, deamination, dihydroxylation and ring-opening induced by vortex cavitation effect.

Acknowledgements

The authors are thankful to Agriculture and Rural Affairs Department of Guangdong Province for providing financial support in the form of Project of Agricultural Scientific Research and Agricultural Technology Extension of Guangdong Province (2021KJ271).

References

- [1] X. Liu, Z. Wang, X.-L. Wang, L. Zhen, C. Yang, E.-H. Li, H.-M. Wei, Status of antibiotic contamination and ecological risks assessment of several typical Chinese surface-water environments, *Huan Jing Ke Xue*, 40 (2019) 2094–2100.
- [2] R. Dagher, P. Drogui, Tetracycline antibiotics in the environment: a review, *Environ. Chem. Lett.*, 11 (2013) 209–227.
- [3] D. Panda, V.K. Saharan, S. Manickam, Controlled hydrodynamic cavitation: a review of recent advances and perspectives for greener processing, *Processes*, 8 (2020) 220, doi: 10.3390/pr8020220.
- [4] G. Mancuso, M. Langone, G. Andreottola, A critical review of the current technologies in wastewater treatment plants by using hydrodynamic cavitation process: principles and applications, *J. Environ. Health Sci. Eng.*, 18 (2020) 311–333.
- [5] K.O. Badmus, J.O. Tijani, E. Massima, L. Petrik, Treatment of persistent organic pollutants in wastewater using hydrodynamic cavitation in synergy with advanced oxidation process, *Environ. Sci. Pollut. Res.*, 25 (2018) 7299–7314.
- [6] S. Raut-Jadhav, D. Saini, S. Sonawane, A. Pandit, Effect of process intensifying parameters on the hydrodynamic cavitation based degradation of commercial pesticide (methomyl) in the aqueous solution, *Ultrason. Sonochem.*, 28 (2016) 283–293.
- [7] V. Innocenzi, M. Prisciandaro, M. Centofanti, F. Vegliò, Comparison of performances of hydrodynamic cavitation in combined treatments based on hybrid induced advanced Fenton process for degradation of azo-dyes, *J. Environ. Chem. Eng.*, 7 (2019) 103171, doi: 10.1016/j.jece.2019.103171.

- [8] G. Li, L. Yi, J. Wang, Y. Song, Hydrodynamic cavitation degradation of Rhodamine B assisted by Fe³⁺-doped TiO₂: mechanisms, geometric and operation parameters, *Ultrason. Sonochem.*, 60 (2020) 104806, doi: 10.1016/j.ultsonch.2019.104806.
- [9] G.L. Chahine, K.M. Kalumuck, Swirling Fluid Jet Cavitation Method and System for Efficient Decontamination of Liquids, PCT/SE2009/050515, 2001.
- [10] H.T. Curt, O.M. Morten, Vortex Generator with Vortex Chamber, PCT/SE2009/050515, 2012.
- [11] J. Wang, X. Wang, P. Guo, J. Yu, Degradation of reactive brilliant red K-2BP in aqueous solution using swirling jet-induced cavitation combined with H₂O₂, *Ultrason. Sonochem.*, 18 (2011) 494–500.
- [12] X. Wang, J. Wang, P. Guo, W. Guo, G. Li, Chemical effect of swirling jet-induced cavitation: degradation of rhodamine B in aqueous solution, *Ultrason. Sonochem.*, 15 (2008) 357–363.
- [13] P. Braeutigam, Z.L. Wu, A. Stark, B. Ondruschka, Degradation of BTEX in aqueous solution by hydrodynamic cavitation, *Chem. Eng. Technol.*, 32 (2009) 745–753.
- [14] B. Wang, R. Zhang, X. Lian, A Swirling Vortex Cavitator, CN 209442699U, 2019.
- [15] K. Soni, K. Jyoti, H. Chandra, R. Chandra, Bacterial antibiotic resistance in municipal wastewater treatment plant; mechanism and its impacts on human health and economy, *Bioresour. Technol. Rep.*, 19 (2022) 101080, doi: 10.1016/j.biteb.2022.101080.
- [16] K.M. Wang, L.X. Zhou, K.F. Ji, S.N. Xu, J.D. Wang, Evaluation of a modified internal circulation (MIC) anaerobic reactor for real antibiotic pharmaceutical wastewater treatment: process performance, microbial community and antibiotic resistance genes evolutions, *J. Water Process Eng.*, 48 (2022) 102914, doi: 10.1016/j.jwpe.2022.102914.
- [17] X. Zhang, H. Yang, Z. Li, Relationship between strength of hydrodynamic cavitation and amount of induced hydroxyl radical, *J. Chem. Ind. Eng.*, 58 (2007) 27–32.
- [18] L. Villeneuve, L. Alberti, J.P. Steghens, J.M. Lancelin, J.L. Mestas, Assay of hydroxyl radicals generated by focused ultrasound, *Ultrason. Sonochem.*, 16 (2009) 339–344.
- [19] X. Wang, J. Jia, Y. Wang, Combination of photocatalysis with hydrodynamic cavitation for degradation of tetracycline, *Chem. Eng. J.*, 315 (2017) 274–282.
- [20] Y.Y. Chen, Y.L. Ma, J. Yang, L.Q. Wang, J.M. Lv, C.J. Ren, Aqueous oxytetracycline degradation by H₂O₂ alone: removal and transformation pathway, *Chem. Eng. J.*, 307 (2017) 15–23.
- [21] S. Yang, Y. Feng, D. Gao, X. Wang, N. Suo, Y. Yu, S. Zhang, Electrocatalysis degradation of oxytetracycline in a three-dimensional aeration electrocatalysis reactor (3D-AER) with a flotation-tailings particle electrode (FPE): physicochemical properties, influencing factors and the degradation mechanism, *J. Hazard. Mater.*, 407 (2021) 124361, doi: 10.1016/j.jhazmat.2020.124361.
- [22] E. Evgenidou, Z. Chatzisalata, A. Tsevis, K. Bourikas, P. Torounidou, D. Sergelidis, A. Koltsakidou, D.A. Lambropoulou, Photocatalytic degradation of a mixture of eight antibiotics using Cu-modified TiO₂ photocatalysts: kinetics, mineralization, antimicrobial activity elimination and disinfection, *J. Environ. Chem. Eng.*, 9 (2021) 105295, doi: 10.1016/j.jece.2021.105295.
- [23] N. Barhoumi, H. Olvera-Vargas, N. Oturan, D. Huguenot, A. Gadri, S. Ammar, E. Brillas, M.A. Oturan, Kinetics of oxidative degradation/mineralization pathways of the antibiotic tetracycline by the novel heterogeneous electro-Fenton process with solid catalyst chalcopyrite, *Appl. Catal., B*, 209 (2017) 637–647.
- [24] R. Delépée, D. Maumeb, B.L. Bizecb, H. Pouliquena, Preliminary assays to elucidate the structure of oxytetracycline's degradation products in sediments. Determination of natural tetracyclines by high-performance liquid chromatography-fast atom bombardment mass spectrometry, *J. Chromatogr. B*, 748 (2000) 369–381.
- [25] S. Zhang, S. Zhao, S. Huang, B. Hu, M. Wang, Z. Zhang, L. He, M. Du, Photocatalytic degradation of oxytetracycline under visible light by nanohybrids of CoFe alloy nanoparticles and nitrogen/sulfur-codoped mesoporous carbon, *Chem. Eng. J.*, 420 (2021) 130516, doi: 10.1016/j.cej.2021.130516.
- [26] Y. Yang, G. Zeng, D. Huang, D. Huang, C. Zhang, D. He, C. Zhou, W. Wang, W. Xiong, X. Li, B. Li, W. Dong, Y. Zhou, Molecular engineering of polymeric carbon nitride for highly efficient photocatalytic oxytetracycline degradation and H₂O₂ production, *Appl. Catal., B*, 272 (2020) 118970, doi: 10.1016/j.apcatb.2020.118970.
- [27] M. Minale, A. Guadie, Y. Li, Y. Meng, X. Wang, J. Zhao, Enhanced removal of oxytetracycline antibiotics from water using manganese dioxide impregnated hydrogel composite: adsorption behavior and oxidative degradation pathways, *Chemosphere*, 280 (2021) 130926, doi: 10.1016/j.chemosphere.2021.130926.
- [28] W. Lai, G. Xie, R. Dai, C. Kuang, Y. Xu, Z. Pan, L. Zheng, L. Yu, S. Ye, Z. Chen, H. Li, Kinetics and mechanisms of oxytetracycline degradation in an electro-Fenton system with a modified graphite felt cathode, *J. Environ. Manage.*, 257 (2020) 109968, doi: 10.1016/j.jenvman.2019.109968.
- [29] J. Ni, D. Liu, W. Wang, A. Wang, J. Jia, J. Tian, Z. Xing, Hierarchical defect-rich flower-like BiOBr/Ag nanoparticles/ultrathin g-C₃N₄ with transfer channels plasmonic Z-scheme heterojunction photocatalyst for accelerated visible-light-driven photothermal-photocatalytic oxytetracycline degradation, *Chem. Eng. J.*, 419 (2021) 129969, doi: 10.1016/j.cej.2021.129969.